JOURNAL OF SPACECRAFT AND ROCKETS
Vol. 49, No. 6, November–December 2012

Sounding Rocket Dispersion Reduction by Second Stage Pointing Control

Frank Scheuerpflug*
DLR, German Aerospace Center, 82234 Oberpfaffenhofen, Germany
Alexander Kallenbach†
Technical University of Munich, 80333 Munich, Germany
and
Francesco Cremaschi‡
Astos Solutions GmbH, 70563 Stuttgart, Germany

DOI: 10.2514/1.A32193

The mission architecture of SHEFEX II features a two-stage solid propellant sounding rocket vehicle on a suppressed trajectory, which is induced by a cold gas pointing maneuver of the vehicle before second stage ignition. The impact point is subject to a 3-σ dispersion of roughly ± 110 km in downrange and ± 90 km in crossrange, which makes a recovery of the vehicle particularly difficult, as the whole impact area is located off shore and the vehicle needs to be recovered by ship. As the major part to dispersion is contributed during the atmospheric ascent of the vehicle, a control algorithm is developed that considers the actual deviation from the nominal trajectory after atmospheric exit and recommends a vehicle pointing that corrects for this deviation. The analytic control algorithm is found by linear/quadratic approximation of the impact point sensitivity towards the deviations after atmospheric exit and to the pointing angles. The effectiveness of the algorithm is tested by implementing it in a full six-degree-of-freedom simulation and applying dispersion factors in a Monte Carlo simulation. The result is a reduction of the impact point dispersion area by about 78%.

Nomenclature

alt	=	altitude, km
$[a, \ldots, f]$	=	constant coefficients
$[m, \ldots, x]$	=	constant coefficients
T_{ref}	=	reference time, s
v	=	velocity, km/s
θ	=	vehicle pitch with respect to vehicle carried north-east-down coordinate system, deg
λ	=	longitude, deg
μ	=	geodetic latitude, deg
ψ	=	vehicle yaw with respect to vehicle carried north-east-down coordinate system, deg

Subscripts

dev	=	deviations
East	=	in east direction relative to rotating earth
GT	=	ground track
I	=	impact
NAP	=	nominal aiming point
North	=	in north direction
ptg	=	pointing
Radial	=	in radial direction

I. Introduction

SHEFEX II (Sharp Edge Flight Experiment) is a reentry technology experiment carried by a two-stage VS-40 sounding rocket and scheduled for launch from Andøya Rocket Range, Norway in June 2012 (see [1]). To maximize the reentry experiment time, a suppressed trajectory is envisaged, featuring an exoatmospheric cold gas pointing maneuver before second stage ignition (see Fig. 1). The rocket motors of both stages are fixed-nozzle design and the vehicle is not equipped with aerodynamic control surfaces. Thus launcher settings, second stage pointing direction and ignition time are the only control parameters to influence the impact point.

Because of limited precision in physics modelling and uncertainties in the actual launch condition as well as the vehicle physical properties, the nominal trajectory can only be met within a certain accuracy and is subject to dispersion. A full six-degree-of-freedom Monte Carlo analysis using the commercial code ASTOS [2], based on 100,000 simulation runs and considering the dispersion factors given in Table 1 leads to a 3-σ impact area of about an elliptical shape, centered about the nominal impact point with semimajor axes 90×110 km (see Fig. 1a). Whereas the second stage contributes only about 10% to the total impact dispersion area, the major contribution originates from the first stage burn and the atmospheric flight. This opens up a possibility to dramatically reduce the impact point dispersion by an adaptive second stage pointing. In this case, the predefined second stage pointing is corrected after first stage burn out and after leaving the relevant atmosphere, thereby considering the deviations caused during the atmospheric ascent and correcting for the most of it by an appropriate second stage pointing.

This document presents and discusses the control strategy derived for the upper stage pointing and the results achieved.

II. Approach

The approach followed herein is to derive an analytical pointing algorithm by an approximation of the second stage pointing corrections required to compensate for any possible deviation from a nominal trajectory.

A. Approximation by Linear/Quadratic Approach

In a first step, the sensitivity of the impact point towards deviations from the nominal flight state at a reference time T_{ref} is raised by a linear function:

Received 5 August 2011; revision received 9 January 2012; accepted for publication 20 January 2012.

*Research Associate, Mobile Rocket Base.

†Aerospace Engineering Student.

‡Senior Engineer.

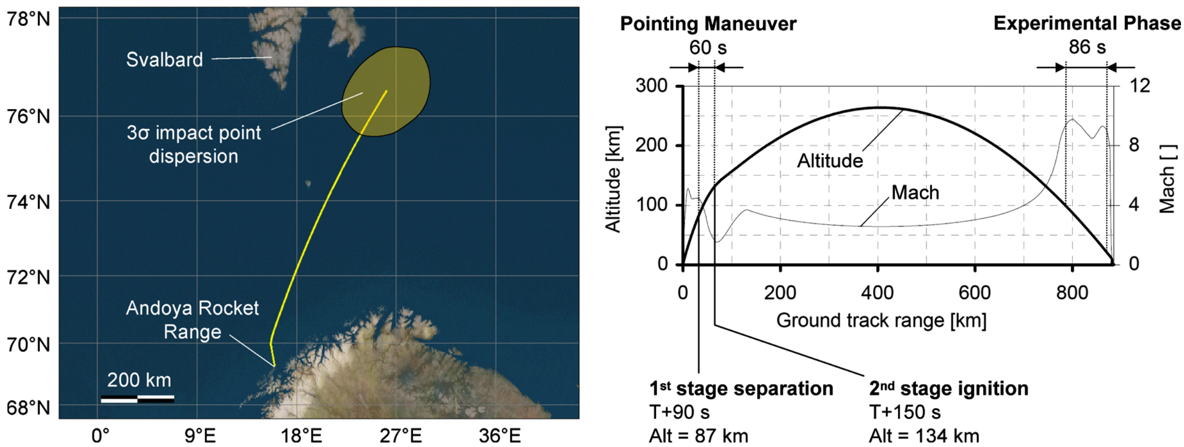

a) Map view **b) Alt vs. ground range**

Fig. 1 SHEFEX II nominal trajectory.

$$\Delta\begin{pmatrix}\mu\\ \lambda\end{pmatrix}_{I,\mathrm{dev}} = \begin{pmatrix} m & n & o & p & q & r\\ s & t & u & v & w & x\end{pmatrix}\cdot\Delta\begin{pmatrix}\lambda\\ \mu\\ \mathrm{alt}\\ v_{\mathrm{North}}\\ v_{\mathrm{East}}\\ v_{\mathrm{Radial}}\end{pmatrix}_{T_{\mathrm{ref}}} \tag{1}$$

This linear correlation implicates the assumption of a Cartesian earth geometry and therefore is valid for impact areas sufficiently small and sufficiently distant from the earth poles. The flight state in Eq. (1) refers to WGS84 coordinates, but other choices of coordinate systems are equally possible. The reference time has to be chosen after first stage burn out and the atmospheric ascent such that dispersion originating from the atmospheric ascent is already introduced into the system. For the mission of SHEFEX II, $T + 90$ s is chosen as the reference time T_{ref}. At this time, the first stage is burnt out and separated and the vehicle has climbed to a nominal altitude of 87.4 km with a 3-σ altitude dispersion of 79.5–93.2 km, which is high enough above the relevant atmosphere in any case. Any of the constant coefficients $[m, \ldots, x]$ are found by introducing one single deviation of the flight state at T_{ref} at a time in the six-degree-of-freedom simulation model, whereas all the others are set to zero. The resulting impact point displacement in relation to the applied magnitude of the deviation yields the coefficient value. For example,

$$\mathrm{m} = \frac{\Delta\mu_{I,\mathrm{dev}}}{\Delta\lambda_{T_{\mathrm{ref}}}} \tag{2}$$

Table 1 3-σ dispersion factors used in analysis

Dispersion factor	3-σ magnitude	Units
First stage burn phase and atmospheric ascent		
Thrust	±3.0	%
Thrust misalignment in pitch axis	±0.1	deg
Thrust misalignment in yaw axis	±0.1	deg
Aerodynamic drag	±20.0	%
Weight	±1.0	%
Fin misalignment	±0.01	deg
Launcher elevation error	±1.0	deg
Launcher azimuth error	±4.0	deg
Head wind	±3.0	m/s
Cross wind	±3.0	m/s
Second stage burn phase and reentry		
Pointing pitch error	±2.0	deg
Pointing yaw error	±2.0	deg
Thrust	±3.0	%
Thrust misalignment in pitch axis	±0.1	deg
Thrust misalignment in yaw axis	±0.1	deg
Aerodynamic drag	±20.0	%
Weight	±1.0	%

To achieve an accurate approximation, the magnitudes of the T_{ref}-deviations assumed have to be close to the maximum deviations expected on the mission. In the presented case, T_{ref}-deviations resulting from the 3-σ dispersion analysis are applied.

Similarly, the sensitivity of the impact point towards the second stage pointing (defined by a pitch angle θ and a yaw angle ψ) is approximated. In the case of pitch dependency, a quadratic approach is applied, as the nominal trajectory is already close to the maximum range of the vehicle and hence the influence of the pitch pointing angle on the impact point is nonlinear:

$$\Delta\begin{pmatrix}\mu\\ \lambda\end{pmatrix}_{I,\mathrm{ptg}} = \begin{pmatrix}\Delta\theta^2\cdot a + \Delta\theta\cdot b + \Delta\psi\cdot c\\ \Delta\theta^2\cdot d + \Delta\theta\cdot e + \Delta\psi\cdot f\end{pmatrix} \tag{3}$$

The coefficients $[a, \ldots, f]$ are found by applying selected values for $\Delta\psi$ and $\Delta\theta$ in the simulation and evaluating the resulting impact point shift. This produces a system of six linear equations which yields the coefficient magnitudes. Ensuring an accurate approximation, the magnitudes assumed for $\Delta\psi$ and $\Delta\theta$ have to be selected such that the resulting impact point shifts are similar in magnitude to the ones from the sensitivity analysis of the impact point with regard to the T_{ref}-deviations. Beside pointing direction, ignition time of the second stage is a possible additional control parameter. It is admittedly unnecessary, having an equivalent influence on the impact point as the pitch angle. For SHEFEX II, an earlier ignition is also not eligible as the operation time for the cold gas pointing system would be inadmissibly shortened. The coefficients resulting from the analysis are given in Table 2.

Table 2 Coefficients for the SHEFEX II mission

Coefficient	Magnitude	Units
m	0.00000	——
n	0.98094	——
o	0.00897	deg /km
p	4.63626	deg /km/s
q	−0.64132	deg /km/s
r	3.64468	deg /km/s
s	1.00000	——
t	0.75281	——
u	0.02421	deg /km
v	4.93585	deg /km/s
w	18.09296	deg /km/s
x	9.66205	deg /km/s
a	−0.00186	1/ deg
b	0.00823	——
c	−0.06185	——
d	−0.00598	1/ deg
e	−0.03451	——
f	0.31149	——

B. Pointing Algorithm

With all coefficients known, the pointing algorithm is derived by demanding that a given shift of the impact point due to deviations during the atmospheric ascent [Eq. (1)] shall be countered by an appropriate pointing correction [Eq. (3)]:

$$\Delta\begin{pmatrix}\mu\\ \lambda\end{pmatrix}_{I,\mathrm{dev}} = -\Delta\begin{pmatrix}\mu\\ \lambda\end{pmatrix}_{I,\mathrm{ptg}} \tag{4}$$

Substituting Eq. (4) into Eq. (3) and resolving the system of two equations by $\Delta\theta$ and $\Delta\psi$ yields the corrections necessary to the pointing:

$$\Delta\theta = \frac{-D \cdot \sqrt{D^2 - 4CE}}{2C} \tag{5}$$

$$\Delta\psi = \frac{-\Delta\mu_{I,\mathrm{dev}} - a\cdot\Delta\theta^2 - b\cdot\Delta\theta}{c} \tag{6}$$

with $\Delta\mu_{I,\mathrm{dev}}$ and $\Delta\lambda_{I,\mathrm{dev}}$ from Eq. (1) and

$$C = c\cdot d - a\cdot f \tag{7}$$

$$D = c\cdot e - b\cdot f \tag{8}$$

$$E = -\Delta\mu_{I,\mathrm{dev}}\cdot f + \Delta\lambda_{I,\mathrm{dev}}\cdot c \tag{9}$$

As a smaller $\Delta\theta$ leads to a flatter trajectory, the negative solution of Eq. (5) is opted for in order to maximize reentry experiment time. The algorithm generally works within broad bounds, and only fails in case the first stage performs far enough below nominal that the nominal aiming point (NAP) gets out of range of the vehicle. In this event, the discriminant of Eq. (5) becomes < 0 and a solution is impossible (neither physically nor mathematically). For the specific mission of SHEFEX II, this event is provoked even by a comparably small underperformance during the atmospheric ascent, as the nominal trajectory already exploits the maximum range performance of the configuration.

C. Pointing Algorithm in Case of Nominal Aiming Point out of Vehicle Range

In this event, the algorithm shall deliver a pointing to an alternative aiming point (AAP) on the nominal ground track that lies in the closest possible vicinity to the NAP (see Fig. 2).

The maximum range of the vehicle is derived from the approximated model in steps: First, the two equations from Eq. (3) are solved for $\Delta\theta$ and $\Delta\psi$:

$$\Delta\theta = \frac{-D \cdot \sqrt{D^2 - 4CE'}}{2C} \tag{10}$$

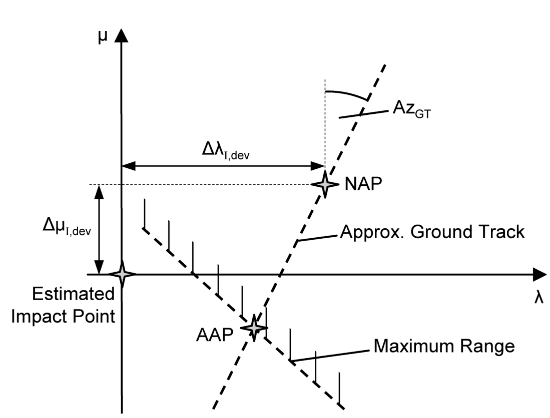

Fig. 2 Finding of AAP.

$$\Delta\psi = \frac{\Delta\mu_{I,\mathrm{ptg}} - a\cdot\Delta\theta^2 - b\cdot\Delta\theta}{c} \tag{11}$$

with

$$E' = \Delta\mu_{I,\mathrm{ptg}}\cdot f - \Delta\lambda_{I,\mathrm{ptg}}\cdot c \tag{12}$$

Second, the discriminant in Eq. (10) is set to zero:

$$\sqrt{D^2 - 4CE'} = 0 \tag{13}$$

Substituting C, D and E' in Eq. (13) and resolving by $\Delta\mu_{I,\mathrm{ptg}}$ yields

$$\Delta\mu_{I,\mathrm{ptg}} = \frac{c}{f}\cdot\Delta\lambda_{I,\mathrm{ptg}} + G \tag{14}$$

with

$$G = \frac{1}{f}\cdot\frac{D^2}{4C} \tag{15}$$

Equation (14) represents a straight line on a map view (see Fig. 2), expressing the maximum range of the vehicle. A second condition is necessary to identify a specific point on this line as the AAP. For SHEFEX II, this is determined to be the intersection between the line of maximum range and a straight line through the NAP that approximates the ground track of the nominal trajectory (see Fig. 2):

$$\Delta\mu_{I,\mathrm{ptg}} = \frac{\cos(\mu_{\mathrm{NAP}})}{\tan(Az_{\mathrm{GT}})}\cdot\Delta\lambda_{I,\mathrm{ptg}} + H \tag{16}$$

with

$$H = -\Delta\mu_{I,\mathrm{dev}} + \Delta\lambda_{I,\mathrm{dev}}\cdot\frac{\cos(\lambda_{\mathrm{NAP}})}{\tan(Az_{\mathrm{GT}})} \tag{17}$$

The AAP is found by setting Eq. (16) equal to Eq. (14) and solving for $\Delta\mu_{I,\mathrm{ptg}}$ and $\Delta\lambda_{I,\mathrm{ptg}}$:

$$\Delta\lambda_{I,\mathrm{ptg}} = \frac{H - G}{(c/f) - [\cos(\lambda_{\mathrm{NAP}})/\tan(Az_{\mathrm{GT}})]} \tag{18}$$

$$\Delta\mu_{I,\mathrm{ptg}} = \frac{c}{f}\cdot\Delta\lambda_{I,\mathrm{ptg}} + G \tag{19}$$

Substituting Eqs. (18) and (19) into Eqs. (10–12) yields the pointing corrections necessary.

III. Results

The presented algorithm is implemented into the ASTOS six-degree-of-freedom simulation and the resulting impact dispersion area is derived by a Monte Carlo simulation, considering the same dispersion factors that are used in the dispersion analysis of the mission with predefined pointing. Figures 3a and 3b show a comparison between the resulting impact point distributions (for clarity only 25,000 impacts displayed). It becomes immediately obvious that a large reduction of the impact area is realized. Analyses with 100,000 runs are the basis to precisely derive the 1-, 2-, and 3-σ dispersion areas, as shown in Figs. 4a and 4b. The reduction in dispersion area achieved by the application of the adaptive pointing algorithm is about 78%. Table 3 gives a comparison of the main dimensions of the 3-σ dispersion areas.

IV. Discussion

It is striking that the shape of the 3-σ dispersion area resulting from an adaptively controlled second stage pointing is strongly asymmetric contrary to the one resulting from a predefined pointing. The adaptive control greatly reduces the dispersion in crossrange and positive downrange, but obviously not in negative downrange. This is owed to the limited vehicle performance, which, in case of an underperformance of the first stage puts the NAP out of reach of the

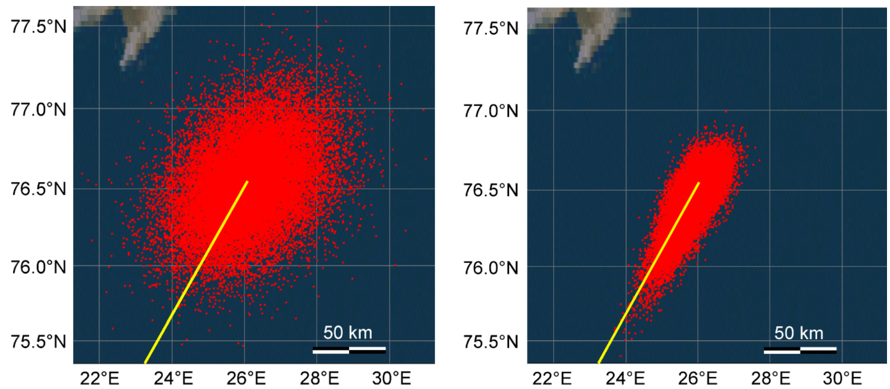

a) Pre-defined pointing **b) Adaptive pointing**

Fig. 3 Comparison of impact point distribution from 25,000 runs Monte Carlo analysis.

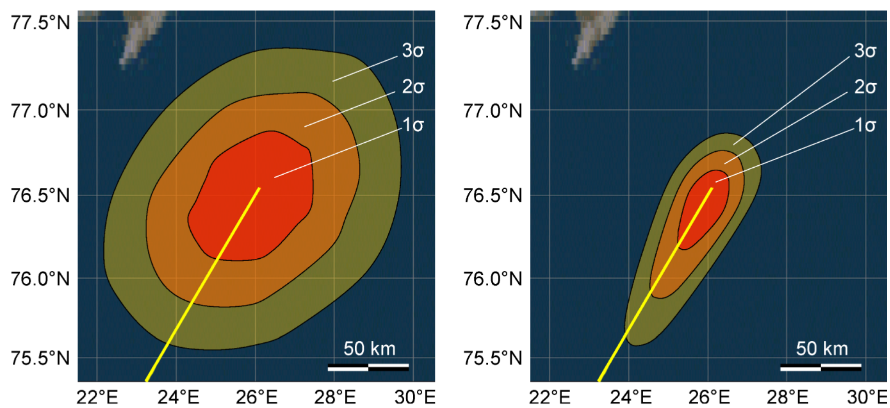

a) Pre-defined pointing **b) Adaptive Pointing**

Fig. 4 Comparison of dispersions derived from a 100,000-run Monte Carlo analysis.

Table 3 Extents of 3-σ dispersion areas resulting from Monte Carlo calculations with and without adaptive second stage pointing control

	$3 - \sigma$ area extent			
Second stage pointing	Positive downrange, km	Negative downrange, km	Positive crossrange, km	Negative crossrange, km
Predefined	100	110	87	84
Adaptive	42	118	22	24

vehicle and can not be compensated for. Therefore, the dispersion reduction achieved with the algorithm presented, would even be better in case of a NAP well within the maximum range of the vehicle.

V. Operational Aspects

From an operational view, it is important to note that the presented algorithm demands that position and velocity data of the vehicle be available at a specific time T_{ref} in order to assess the actual deviations from a nominal trajectory. To accord the algorithm with robustness to a possible system or telemetry dropout induced unavailability of vehicle data at T_{ref}, another small algorithm was implemented that calculates the flight state at T_{ref} from any other flight state by a simple ballistic three-degree-of-freedom model. For SHEFEX II, the presented algorithm is implemented in the ground segment. This is due to the architecture of the onboard computer, but also allows for a human decision on the flight status data source of the algorithm (Global Positioning System or inertial measurement unit).

VI. Conclusions

A robust, low cost method for reducing the impact point dispersion of SHEFEX II has been developed, and is in principle applicable to any other sounding rocket mission that features an exoatmospheric upper stage ignition. The only prerequisites are the existence of an attitude determination and an attitude control system, which in case of SHEFEX II has been implemented mainly in order to achieve a suppressed trajectory design, but now has also been exploited to improve trajectory accuracy and ease recovery operations as well as telemetry coverage. In contrast to common means of dispersion reduction, like thrust vector control or aerodynamic control surfaces, the presented method of upper stage pointing control is easily realizable without adding any complex subsystem to the vehicle.

References

[1] Weihs, H., Longo, J., and Turner, J., "The Sharp Edge Flight Experiment SHEFEX II, a Mission Overview and Status," *Proceedings of the 15th AIAA International Space Planes and Hypersonic Systems and Technologies Conference*, 2008.

[2] Cremaschi, F., Weikert, S., Wiegand, A., and Scheuerpflug, F., "Sounding Rocket Trajectory Simulation and Optimization With ASTOS," *Proceedings of the 19th ESA Symposium on European Rocket and Balloon Programmes and Related Research*, 2009.

D. Geller
Associate Editor